Thermochimica Acta, 170 (1990) 19–33
Elsevier Science Publishers B.V., Amsterdam

ACTIVATION ENERGY DETERMINATION FROM DIELECTRIC THERMAL ANALYSIS

KIRK A. NASS * and JAMES C. SEFERIS **

Polymeric Composites Laboratory, Department of Chemical Engineering, BF-10, University of Washington, Seattle, WA 98195 (U.S.A.)

(Received 5 February 1990)

ABSTRACT

A new method is presented for calculating the activation energy of relaxation transitions in polymers, such as the glass transition, from isofrequency dielectric measurements. The method incorporates a two-parameter model to describe mathematically the dielectric properties during the transition. An Arrhenius expression was used to describe the temperature dependence of the dielectric relaxation time. The technique was used to determine experimentally the activation energy of the glass transition of an uncured epoxy–amine model resin, tetraglycidyl-4,4′-diaminodiphenylmethane with 25 parts per hundred of 4,4′-diaminodiphenylsulfone hardener, for high performance polymeric composites. The results were comparable with those obtained using traditional multifrequency methods.

INTRODUCTION

Traditional thermal analysis techniques, such as differential scanning calorimetry (DSC), dynamic mechanical analysis (DMA), and thermogravimetric analysis (TGA), provide quantitative information about the physical and chemical processes which occur in polymers and polymeric composites either during processing or under performance conditions. Electrical property changes, which also occur during transitions, may be detected by alternating current methods, thus providing additional means of obtaining the physicochemical information available via standard thermal analysis [1].

Interest in dielectric measurements of polymeric systems has increased by the recent availability of commercial dielectric measuring equipment, such as the Du Pont 2970 dielectric analyzer, the Tetrahedron ADR-380 automatic dielectric rheometer, and the Micromet Eumetrics II dielectrometer, among others. Although these instruments are adequate for application of

* Current address: Chevron Research and Technology Company, P.O. Box 1627, Richmond, CA 94802-0627, U.S.A.
** Author to whom correspondence should be addressed.

0040-6031/90/$03.50

dielectrics to polymer characterization, current research efforts have focused on monitoring and control applications [2–6]. However for all applications, irrespective of the instrument used, the development of quantitative techniques for extracting physicochemical parameters, such as activation energies from dielectric data, is required if further application of this technique as a thermoanalytical tool is to be developed.

In this paper, a new method for calculating the activation energy for any type of dielectric transition is presented and used to analyze the dielectric properties of a model high performance thermosetting resin going through its uncured glass transition. This supplements our earlier studies on the use of dielectrics in obtaining cure reaction activation energies for the same systems [2,3,5]. The success of the new technique is demonstrated by comparing these results with those determined using established viscoelastic property data analysis methods. In this work, classical thermoanalytical expressions are developed for calculating reaction activation energies from the dielectric properties of polymers during isothermal and non-isothermal conditions.

BACKGROUND

Dielectric spectroscopy measures the response of materials to a sinusoidal electric field, E^*, in analogous fashion to dynamic mechanical analysis which measures the response to a sinusoidal stress or strain. The dielectric constant, ϵ^*, is defined as the proportionality constant between the applied electric field, E^*, and the resulting electric displacement, D^*:

$$D^* = \epsilon^* E^* \tag{1}$$

The dielectric constant may be expressed in terms of its real and imaginary components:

$$\epsilon^* = \epsilon' - i\epsilon'' \tag{2}$$

In physical terms, the value of ϵ' is related to the amount of electric energy stored in the material, and hence ϵ' is termed the "storage component". The value of ϵ'', the "loss component" of the dielectric constant, is proportional to the amount of electric energy dissipated by the material.

The storage and loss components are calculated from experimental measurements of the capacitance, C, and dissipation ($\tan \delta$), which for parallel plate electrodes gives

$$\epsilon' = \frac{Cd}{Ae_0} \tag{3}$$

The phase angle δ can be measured directly by comparing the input and

output AC phases. Since $\tan \delta = \epsilon''/\epsilon'$, the loss component ϵ'' can be easily calculated as

$$\epsilon'' = \epsilon' \tan \delta \tag{4}$$

In the equations above, A (cm^2) is the electrode area, d (cm) is the electrode spacing, and e_0 (8.854×10^{-14} F cm^{-1}) is the permittivity of free space. When single-surface interdigitated electrodes are used to measure the dielectric properties, as with the Du Pont 2970 dielectric analyzer and the Micromet Eumetrics II dielectrometer, ϵ' and ϵ'' are determined by comparing the electric response with calibration tables stored in the instrument's memory [7].

The glass transition (the transformation of polymers from glassy to rubbery states) is easily detected as a distinct change in the viscoelastic properties, such as creep compliance or stress relaxation modulus, when plotted as functions of temperature. Transitions observed at temperatures below the glass transition temperature have been correlated with relaxations associated with molecular segments of the polymeric chain [8]. The time scale of the relaxation determines the frequency behavior of the transition when observed using dynamic techniques, such as dynamic mechanical analysis.

The relaxation of dipolar segments of the molecules causes distinct changes in the dielectric properties of polymers [1]. For systems that

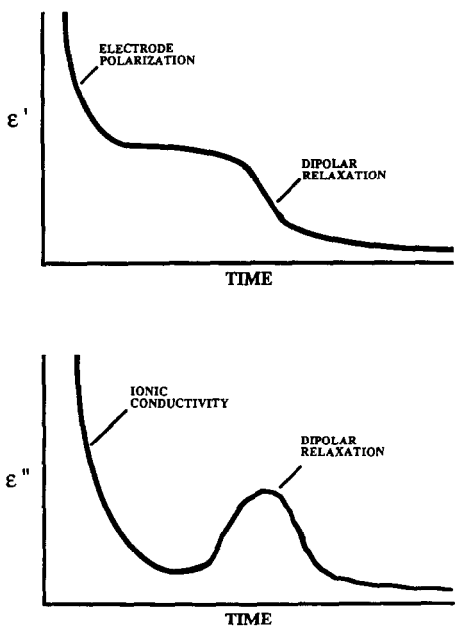

Fig. 1. Typical isofrequency dielectric responses of thermosetting polymers during isothermal cure.

undergo chemical reactions (cure) during the experiment, the dielectric transitions will manifest themselves differently, depending on experimental conditions and the physical state of the sample. Representative dielectric property changes during use of a thermosetting polymer are plotted as functions of temperature in Fig. 1. For each frequency, the value of ϵ'' reaches a maximum which shifts to higher temperatures at higher frequencies. The value of ϵ' decreases during cure, passing through an inflection point which corresponds to the position of ϵ'' maximum. The activation energy is characterized by analyzing the frequency (dispersion) and temperature behavior, of the dielectric properties during the observed dielectric transitions.

DIPOLAR RELAXATION: FREQUENCY AND TEMPERATURE DEPENDENCE

The dispersion behavior of non-reacting polymers is observed in complex plane (Cole–Cole) plots of the dielectric properties [1]. In these curves of ϵ'' plotted against ϵ', each data point corresponds to the dielectric properties at a fixed frequency. The curves have been described mathematically as functions of the product of angular frequency, ω (rad s^{-1}), and the dipolar relaxation time, τ.

Ideal polymer dispersion behavior has been described using a single dipolar relaxation time, τ_0. The complex dielectric constant, ϵ^*, may be related to the product $\omega\tau_0$ by the Voigt equation [1]

$$\epsilon^* = \epsilon_\infty + \frac{\epsilon_0 - \epsilon_\infty}{1 + i\omega\tau_0} \tag{5}$$

where ϵ_0 and ϵ_∞ are the values of ϵ' at $\omega = 0$ and ∞. When rearranged and expressed in terms of ϵ' and ϵ'', eqn. (5) describes a semicircle centered on the ϵ' axis at $(\epsilon_0 + \epsilon_\infty)/2$, as shown in Fig. 2. The maximum value of ϵ'' occurs at $\omega\tau_0 = 1$.

Real polymers, however, are polydisperse and heterogeneous systems which possess distributions of relaxation times. Therefore, the experimental dispersion curves of polymers may be either broader than the ideal curve or asymmetric at high frequencies, or both. A generalized equation proposed by Havriliak and Negami produces the full range of polymer dispersion curves using the two parameters α and β, and the mean dipolar relaxation time, τ [9,10]:

$$\epsilon^* = \epsilon_\infty + \frac{\epsilon_0 - \epsilon_\infty}{\left[1 + (i\omega\tau)^{1-\alpha}\right]^\beta} \tag{6}$$

where

$$0 \leqslant \alpha \leqslant 1 \qquad 0 \leqslant \beta \leqslant 1 \tag{7}$$

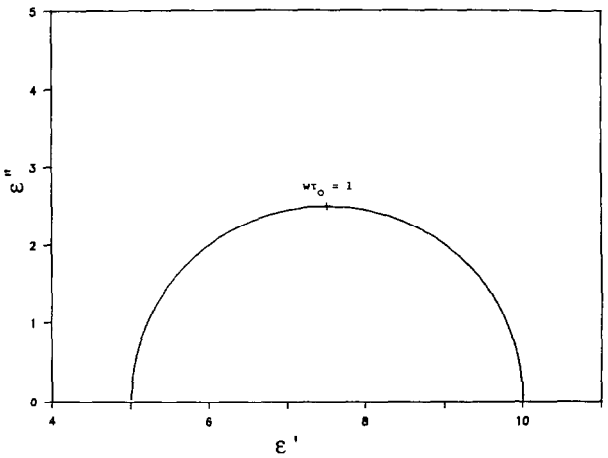

Fig. 2. Complex plane plot of Voigt model, with $\tau_0 = 0.1$ s, $\epsilon_0 = 10$, $\epsilon_\infty = 5$.

Expressions for ϵ' and ϵ'' in terms of $\omega\tau$ are obtained from eqn. (6) by a successive application of De Moivre's theorem of complex variable theory:

$$\epsilon' = \epsilon_\infty + \frac{(\epsilon_0 - \epsilon_\infty)\cos(\beta\phi)}{\left\{1 + 2(\omega\tau)^{1-\alpha}\cos[(1-\alpha)\pi/2] + (\omega\tau)^{2(1-\alpha)}\right\}^{\beta/2}} \tag{8}$$

$$\epsilon'' = \frac{(\epsilon_0 - \epsilon_\infty)\sin(\beta\phi)}{\left\{1 + 2(\omega\tau)^{1-\alpha}\cos[(1-\alpha)\pi/2] + (\omega\tau)^{2(1-\alpha)}\right\}^{\beta/2}} \tag{9}$$

where ϕ is defined by

$$\phi = \tan^{-1}\left\{\frac{(\omega\tau)^{1-\alpha}\sin[(1-\alpha)\pi/2]}{1 + (\omega\tau)^{1-\alpha}\cos[(1-\alpha)\pi/2]}\right\} \tag{10}$$

The dispersion behavior described by these equations is plotted in Fig. 3. The α parameter produces broadening and β produces high frequency asymmetry. Ideal dispersion behavior is produced by values of α approaching 0 and β approaching 1. Values of α and β may be determined from dielectric data through a combination of graphical and iteration methods [9,11,12]. Several features of the dispersion behavior in Fig. 3 are worth noting. The angle formed by the intersection of the high frequency tail with the ϵ' axis, ϕ_L, is related to α and β by

$$\varphi_L = (1-\alpha)\beta(\pi/2) \tag{11}$$

The maximum value of ϵ'' does not occur when $\omega\tau = 1$, as with symmetric dispersions. The condition of $\omega_t = 1$ occurs at the intersection of the bisector of ϕ_L with the dispersion curve, as illustrated in Fig. 3.

The exact physical significance of the dispersion parameters has not yet been established. Efforts to interpret the parameters in molecular terms have

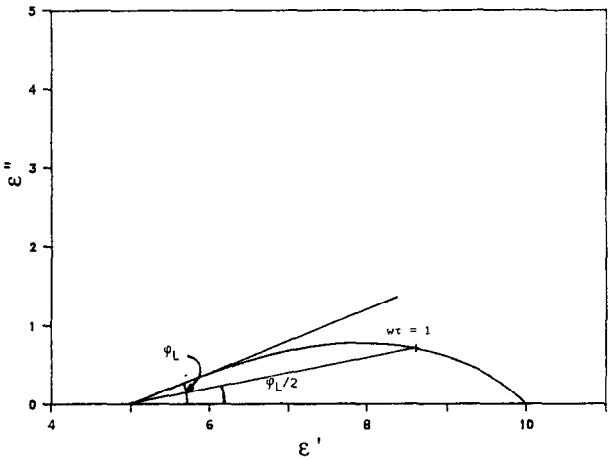

Fig. 3. Complex plane plot of Havriliak–Negami equation, with $\tau = 0.1$ s, $\epsilon_0 = 10$, $\epsilon_\infty = 5$.

begun through statistical experimental design [13,14]. The equations may still be used, however, to determine accurately the activation energy of dielectric transitions.

If assumed to be an activated process, the temperature behavior of dipolar relaxation can be described by an Arrhenius expression [1]:

$$\tau = \tau' \exp(E_\tau / RT) \tag{12}$$

where τ' is the pre-exponential constant, R is the gas constant, and E_τ represents the activation energy of the transition. Thus the key to determining the transition activation energy from dielectric data is in combining eqn. (12) with the appropriate dispersion relationship.

TRANSITION ACTIVATION ENERGY

Two methods relate the activation energy of a dielectric transition to either the area or the half-width of ϵ'' curves plotted as a function of $1/T$ [1]. Each method, however, applies only to symmetric dispersion behavior. A third method, the peak temperature method, is valid for any type of dispersion. This method assumes that the maximum value of ϵ'' for each frequency occurs when $\omega\tau$ reaches a unique value. At a given temperature, the frequency at which ϵ'' is a maximum is denoted as ω_{max}. Alternatively, the temperatures at which ϵ' data exhibit an inflection for each frequency may be used to determine ω_{max} [15].

Under the uniqueness assumption and eqn. (12), Arrhenius curves of ω_{max} should be linear. The transition activation energy may be calculated as [8]

$$E_\tau \approx -R \frac{\mathrm{d}(\ln \omega_{max})}{\mathrm{d}(1/T)} \tag{13}$$

This method is applicable to both symmetric and asymmetric dispersions since the ϵ'' maximum occurs when $\omega\tau$ reaches a value that is characteristic of the dispersion type, e.g. $\omega\tau = 1$ for symmetric dispersions. However, dielectric data must be obtained over a wide range of frequencies to obtain an accurate value of E_τ.

DIELECTRIC LOSS METHOD

In this study, an alternative method was developed for calculating the transition activation energy for any type of dispersion behavior from iso-frequency dielectric data. The method calculates the activation energy from Arrhenius-type plots of the ratios of ϵ'' values to the maximum ϵ''_m value and the appropriate values of the dispersion parameters. For a given frequency, ϵ''_m for a transition calculated from the Havriliak–Negami relation (eqn. (6)) gives

$$\epsilon''_m = \frac{(\epsilon_0 - \epsilon_\infty)\sin(\beta\phi_m)}{\left\{1 + 2(\omega\tau_m)^{1-\alpha}\cos[(1-\alpha)\pi/2] + (\omega\tau_m)^{2(1-\alpha)}\right\}^{\beta/2}} \tag{14}$$

The values of the relaxation time and ϕ at ϵ''_m were denoted as τ_m and ϕ_m respectively. Dividing eqn. (9) by eqn. (14) and rearranging produces the ratio of ϵ'' to ϵ''_m:

$$\frac{\epsilon''}{\epsilon''_m} = \frac{1}{A}\,\frac{\sin(\beta\phi)}{\left\{1 + 2(\omega\tau)^{1-\alpha}\cos[(1-\alpha)\pi/2] + (\omega\tau)^{2(1-\alpha)}\right\}^{\beta/2}} \tag{15}$$

where

$$A = \frac{\sin(\beta\phi_m)}{\left\{1 + 2(\omega\tau_m)^{1-\alpha}\cos[(1-\alpha)\pi/2] + (\omega\tau_m)^{2(1-\alpha)}\right\}^{\beta/2}} \tag{16}$$

which is simply a function of frequency. The values of α and β were assumed to be independent of temperature. While both α and β have been observed to vary with temperature, the temperature ranges of transition are typically small enough that these parameters may be assumed constant [10]. Under this assumption, A may be considered constant during the observed dielectric transition.

If it is considered that, at temperatures above the ϵ''_m temperature,

$$(\omega\tau)^{1-\alpha} \ll 1$$

therefore

$$\frac{(\omega\tau)^{1-\alpha}\sin[(1-\alpha)\pi/2]}{1 + (\omega\tau)^{1-\alpha}\cos[(1-\alpha)\pi/2]} \ll 1$$

In addition, for $x \ll 1$, $\tan^{-1}(x) \approx x$. From eqn. (10), the value of ϕ above the peak transition temperature simplifies to

$$\phi \approx \frac{(\omega\tau)^{1-\alpha} \sin[(1-\alpha)\pi/2]}{1 + (\omega\tau)^{1-\alpha} \cos[(1-\alpha)\pi/2]} \tag{17}$$

Since $\beta < 1$ and $\phi \ll 1$, the product $\beta\phi$ is also much less than unity. The numerator in eqn. (15) simplifies to

$$\sin(\beta\phi) \approx \beta\phi \approx \frac{\beta(\omega\tau)^{1-\alpha} \sin[(1-\alpha)\pi/2]}{1 + (\omega\tau)^{1-\alpha} \cos[(1-\alpha)\pi/2]} \tag{18}$$

This equation may be simplified further by recognizing that, for $\omega\tau$ less than 1,

$$(\omega\tau)^{1-\alpha} \cos[(1-\alpha)\pi/2] \ll 1$$

and therefore

$$\sin(\beta\phi) \approx \beta\phi \approx \beta(\omega\tau)^{1-\alpha} \sin[(1-\alpha)\pi/2] \tag{19}$$

The denominator in eqn. (15) can also be simplified to unity since, for α and $\omega\tau$ less than 1,

$$2(\omega\tau)^{1-\alpha} \cos[(1-\alpha)\pi/2] + (\omega\tau)^{2(1-\alpha)} \ll 1 \tag{20}$$

Substituting eqns. (19) and (20) into eqn. (15) yields an expression for the ratio of ϵ'' values above the transition temperature to the peak value, ϵ''_m:

$$\frac{\epsilon''}{\epsilon''_m} = \frac{\beta(\omega\tau)^{1-\alpha} \sin[(1-\alpha)\pi/2]}{A} \tag{21}$$

Taking the logarithm of both sides produces:

$$\ln\frac{\epsilon''}{\epsilon''_m} = \ln\frac{\beta \sin[(1-\alpha)\pi/2]}{A} + (1-\alpha) \ln(\omega\tau) \tag{22}$$

The final equation relating the activation energy to the ratio of ϵ'' to ϵ''_m was obtained by incorporating the Arrhenius expression for τ, eqn. (12), into eqn. (22):

$$\ln\frac{\epsilon''}{\epsilon''_m} = \ln\frac{\beta \sin[(1-\alpha)\pi/2]}{A} + (1-\alpha) \ln(\omega\tau') + \frac{(1-\alpha)E_\tau}{RT} \tag{23}$$

Equation (23) predicts that Arrhenius plots of post-transition values of ϵ''/ϵ''_m should be linear. The activation energy is calculated as

$$E_\tau = \frac{R}{1-\alpha} \frac{d[\ln(\epsilon''/\epsilon''_m)]}{d(1/T)} \tag{24}$$

for $\epsilon'' < \epsilon''_m$.

The mathematical assumptions in the method development were tested by using eqn. (24) to calculate the activation energy of a model dielectric

TABLE 1

Comparison of activation energy calculations: uncured TGDDM–DDS (25 phr)

Heating rate (°C min^{-1})	E_a (kcal mol^{-1})					
	ω_{max} method	ϵ'' ratio method				
		1 kHz	2 kHz	4 kHz	10 kHz	20 kHz
1	44.51	– [a]	48.97	48.86	47.00	45.01
5	41.70	40.24	36.64	46.14	42.89	43.05
10	(29.85)	34.79	40.86	39.14	41.60	43.52
Average	43.11	37.52	42.16	44.71	43.83	43.86

[a] Maximum in ϵ'' occurred below 30 °C.

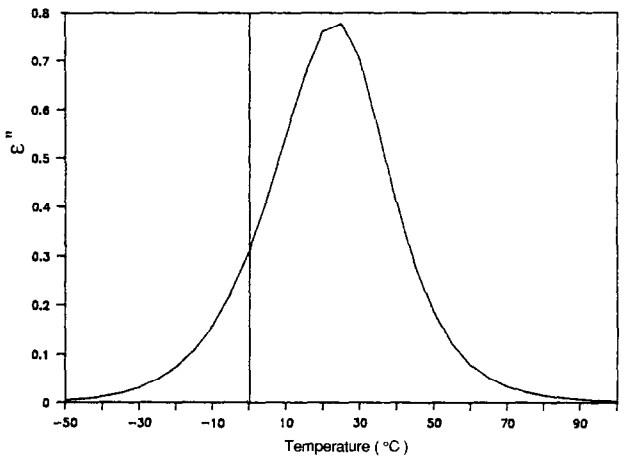

Fig. 4. Model dielectric transition generated by Havriliak–Negami equation and model parameter values.

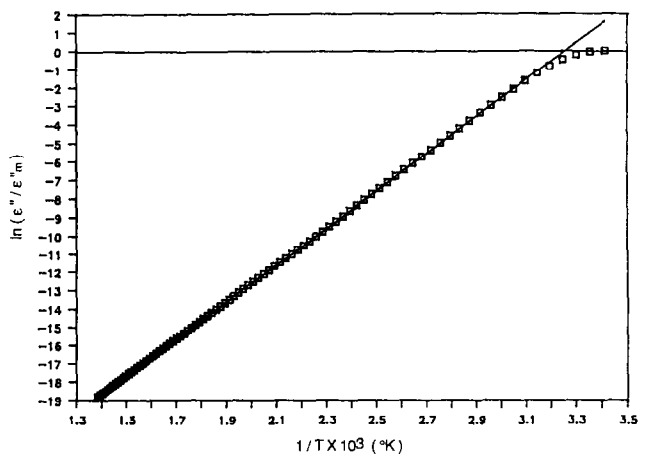

Fig. 5. Arrhenius plot of ϵ'' ratios from model Havriliak–Negami transition.

transition. Model transition data were generated using eqns. (8), (9), and (12), and representative dispersion parameter values. An arbitrary activation energy of 40.00 kcal mol^{-1} was used. Figure 4 contains the generated ϵ'' values plotted as functions of temperature. An Arrhenius plot of the ϵ'' ratios in Fig. 5 exhibits the expected linearity at temperatures above the peak transition temperature. The activation energy calculated from the slope of the line in Fig. 5 and eqn. (24) is 39.91 kcal mol^{-1}. The agreement between this and the "real" value validates the assumptions, permitting the calculation of dielectric transition activation energies from isofrequency dielectric data.

As outlined above, eqns. (13) and (24) allow calculations of the activation energy in dielectric transitions to be determined. The success in applying these methods to real dielectric data was demonstrated by calculating the activation energies of transition for a model thermosetting resin system.

EXPERIMENTAL

Model thermosetting resin

The resin used in the study was a high performance resin consisting of a tetrafunctional epoxy, tetraglycidyl-4,4′-diaminodiphenylmethane (TGDDM; $M_w = 422.49$) cured with a tetrafunctional amine hardener 4,4′-diaminodiphenylsulfone (DDS; $M_w = 248.31$). The resin composition used 25 parts per hundred epoxy (phr) DDS, an epoxy-rich mixture of 43% amine stoichiometry.

TGDDM and DDS were obtained commercially as Ciba–Geigy MY 720 and Ciba–Geigy HT 976 and were used as received. The resin mixture was prepared to ensure homogeneous mixing without pre-reaction [16]. TGDDM was first heated to 135 °C in an oil bath and stirred for an additional 5 min, removed from the oil bath, degassed at 95 °C under 30 mmHg vacuum for 30 min, and stored at −10 °C to prevent pre-reaction. Precautions were taken to minimize resin exposure to moisture.

Dielectric equipment

The resin cure was monitored using a previously designed disposable two-terminal parallel-plate dielectric cell [17]. A General Radio 1688 precision digibridge, controlled by a Hewlett–Packard 9000 computer, measured the capacitance and dissipation of the resin during the cure. Values of ϵ' and ϵ'' were calculated in real time from the electric properties, electrode geometry, and eqns. (3) and (4).

Samples of TGDDM–DDS resin were monitored during non-isothermal heating using a smaller version of the two-terminal dielectric cell. Non-iso-

thermal temperature control was made possible by performing the experiments in the heating chamber of a Du Pont 982 dynamic mechanical analyzer (DMA) controlled by Du Pont 1090 and/or 2000 thermal analyzer systems. The dielectric cell was placed in the DMA sample area with the radiative heat shield installed. The DMA thermocouple was placed flush against the sample to minimize thermal lag between the sample and the programmed chamber temperature. The dielectric properties of the TGDDM–DDS system were monitored at 240 Hz, 1 kHz, 4 kHz, 10 kHz, and 20 kHz during constant heating from 30 °C at 1, 5, and 10 °C min^{-1}. Some selected experimental results were also validated and reproduced with the recently developed Du Pont Dielectric Analyzer System (DEA).

RESULTS AND DISCUSSIONS

The dielectric properties measured below the onset of polymerization of the TGDDM–DDS resin are presented in Figs. 6–8. The glass transition temperature, T_g, measured by DSC for an uncured mixture of TGDDM and 25 phr DDS, was −7 °C. In addition, the dielectric properties at these temperatures follow those expected during a typical dielectric transition. Therefore, the frequency-dependent changes in ϵ' and ϵ'' just above room temperature result from the subsistence of the uncured glass transition temperature. The activation energy of the uncured TGDDM–DDS glass transition was calculated from the dielectric data using both the ω_{max} and ϵ'' ratio methods.

As required by the ω_{max} method, Arrhenius plots of the peak transition frequencies were constructed for each set of heating rate data, as seen in Fig.

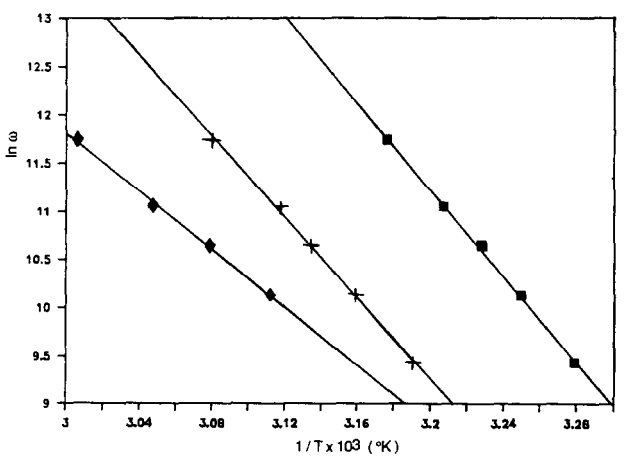

Fig. 6. Arrhenius plots of peak frequencies as a function of $1/T$ for uncured TGDDM–DDS (25 phr) at 1 °C min^{-1} (■), 5 °C min^{-1} (+) and 10 °C min^{-1} (◆).

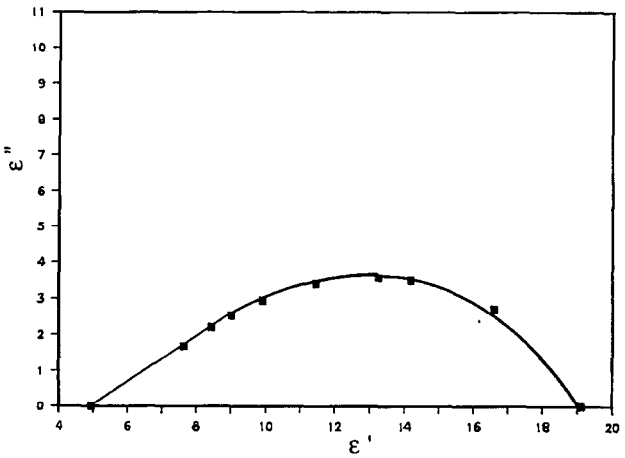

Fig. 7. Complex plane plot of dielectric properties of uncured TGDDM–DDS at 30.65 °C.

6. The activation energies calculated from these curves are summarized in Table 1. The exceptionally low value of E_τ at 10 °C min^{-1} is probably due to thermal lag at the beginning of the experiment, when the glass transition is coincidentally observed.

Before applying the ϵ'' ratio method to the dielectric data, the Havriliak–Negami dispersion parameters were determined for the TGDDM–DDS uncured glass transition. Figure 7 is an example of the isothermal complex plane plot of the dielectric properties at 30.7 °C. From the slope of the high frequency portion of the dispersion curve and procedures outlined elsewhere, values of $\alpha = 0.273$ and $\beta = 0.487$ were calculated

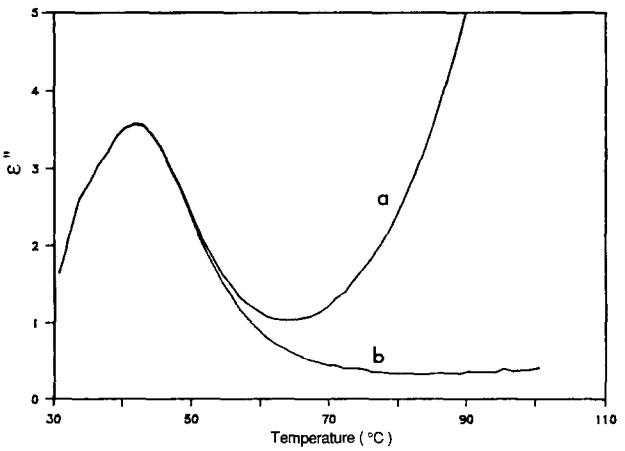

Fig. 8. Low temperature 20 kHz dielectric loss ϵ'' of uncured TGDDM–DDS at 1 °C min^{-1}: a, experimental; b, conduction subtracted.

[9]. These values were assumed to be constant with temperature and independent of the heating rate.

Since the dielectric loss method holds only for dipolar relaxation during transition, the contribution from ionic conduction was removed from the dielectric data using the following procedure. Dielectric data obtained at 240 Hz, which may be dominated by conductive effects, were used to calculate the conductivity during transition and hence to obtain conductivity-free values of ϵ'' at other frequencies. The apparent conductivity was calculated from the frequency and the value of ϵ'' [1]:

$$\sigma = \epsilon'' \omega e_0 \tag{25}$$

Here σ is the apparent conductivity, and e_0 is the permittivity of free space, 8.854×10^{-14} F cm^{-1}. The resin conductivity was calculated from the 240 Hz data at temperatures higher than the detected glass transition and was subtracted from the ϵ'' data for other frequencies according to the following expression:

$$\epsilon''_{\text{dipolar}}(\omega) = \epsilon''(\omega) - \frac{\epsilon''(240 \text{ Hz}) \times 240}{f} \tag{26}$$

where f is the frequency. An example of ϵ'' data at 20 kHz with and without conductivity effects is given in Fig. 8. The isofrequency conduction-free ϵ'' data were then ratioed to the maximum value and plotted in Arrhenius fashion, as shown in Fig. 9. The activation energies calculated from the slopes of the curves for each frequency are summarized in Table 1.

These values show good agreement with those calculated by the $\omega_{\max}$ method at 1 and 5 °C min^{-1}, differing by only a few per cent. The excellent agreement between the values of E_τ calculated at each frequency validates the model assumptions. Therefore, the dielectric loss method may be used to

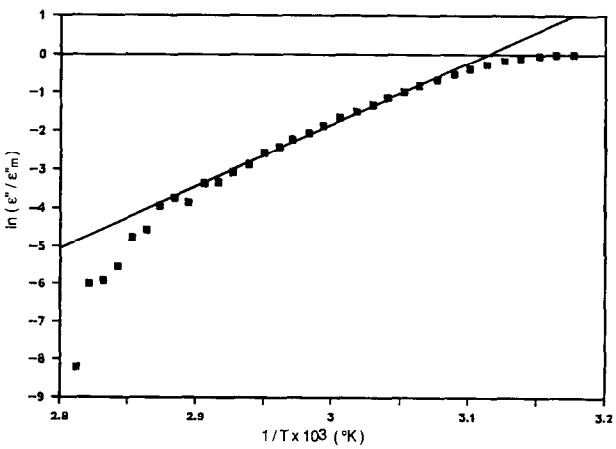

Fig. 9. Arrhenius plot of 20 kHz ϵ''/ϵ''_m ratios for TGDDM–DDS glass transition.

determine dielectric transition activation energies. Dielectric thermal analysis techniques such as these have a distinct advantage over other viscoelastic property measurement methods since the dielectric properties of both uncured and cured polymer systems may be measured with the same apparatus.

CONCLUSIONS

A new method has been developed for determining the activation energy of dielectric transition from dielectric data. This method assumes that the inflection in ϵ' and the simultaneous peak in ϵ'' during transition occur at unique values of the relaxation time for each frequency. The method is based on the frequency dependence of polymeric dielectric properties described by the Havriliak–Negami dispersion equation. This method allows ϵ_τ to be calculated from isofrequency ϵ'' data and the appropriate values of the dispersion parameters. The dielectric loss method was experimentally validated by analyzing the glass transition of uncured TGDDM–DDS resin. The average values calculated from the dielectric properties at the examined frequencies were in excellent agreement with the value calculated using the ω_{max} method.

The success of using dielectric spectroscopy to determine the activation energies of polymeric systems has been demonstrated. A further step in developing dielectric thermal analysis techniques is the description of reaction activation energy from dielectric properties during cure.

ACKNOWLEDGMENTS

The authors would like to acknowledge Drs. M.A. Bachmann of ICI and E.M. Woo of the Polymeric Composites Laboratory for helpful discussions in the development of this technique. Support for this project was provided by Tetrahedron Associates and Du Pont Instruments, through equipment support to the Polymeric Composites Laboratory consortium at the University of Washington, and the National Science Foundation and ICI through the Presidential Young Investigator Award to Professor J.C. Seferis.

REFERENCES

1 N.G. McCrum, B.E. Read and G. Williams, Anelastic and Dielectric Effects in Polymeric Solids, Wiley, London, 1967.
2 K.A. Nass and J.C. Seferis, Polym. Eng. Sci., 29 (1989) 3115.
3 K.A. Nass, J.C. Seferis and M.A. Bachmann, Proc. Annu. Tech. Conf. Soc. Plast. Eng., 33 (1987) 1047.

4 W.W. Bidstrup and S.D. Senturia, Proc. Annu. Tech. Conf. Soc. Plast. Eng., 34 (1988) 960.
5 W.M. Sanford and R.L. McCullough, Proc. Annu. Tech. Conf. Am. Soc. Compos., 2 (1987) 21.
6 K.A. Nass, Ph.D. Dissertation, Department of Chemical Engineering, University of Washington, 1989.
7 T. Grentzer and J. Leckenby, Am. Lab., 21 (1989) 82.
8 I.M. Ward, Mechanical Properties of Solid Polymers, Wiley–Interscience, New York, 2nd edn., 1983.
9 S. Havriliak and S. Negami, J. Polym. Sci., Part C, 14 (1966) 99.
10 S. Havriliak and S. Negami, Polymer, 8 (1967) 161.
11 J.W. Lane, M.S. Thesis, Department of Chemical Engineering, University of Washington, 1984.
12 J.W. Lane, J.C. Seferis and M.A. Bachmann, J. Appl. Polym. Sci., 31 (1986) 1155.
13 S. Havriliak and D.G. Watts, Polymer, 27 (1986) 1509.
14 Y. Zhu and D.G. Watts, Polymer, 29 (1988) 325.
15 G. Banhegyi, P. Hedvig and F.E. Karasz, J. Appl. Polym. Sci., 35 (1988) 679.
16 H.S. Chu and J.C. Seferis, in J.C. Seferis and L. Nicolais (Eds.), The Role of the Polymer Matrix on the Processing and Structural Properties of Composite Materials, Plenum, New York, 1989.
17 J.W. Lane, J.C. Seferis and M.A. Bachmann, Polym. Eng. Sci., 26 (1986) 34.